CHAOTIC COEXISTENCE IN A TOP-PREDATOR MEDIATED COMPETITIVE EXCLUSIVE WEB

BRIAN BOCKELMAN, BO DENG, ELIZABETH GREEN, GWENDOLEN HINES, LESLIE LIPPITT, AND JASON SHERMAN

ABSTRACT. A basic food web of 4 species is considered, of which there is a bottom prey X, two predators Y, Z on X, and a top predator W only on Y. The study concerns with how one type of chaotic coexistence arises. It is shown that under the situation that without the top-predator W, competitor Z goes to extinction, without Z the XYW locks in a periodic cycle, yet with all species, the noncompetitive Z can derive the dynamics from periodic orbits to chaos. The dynamics can be captured analytically by 1-dimensional unimodal and multimodal maps and symbolic shift maps.

Dedicated to Prof. S.-H. Chow For The Celebration of His Sixtieth Birthday

1. Introduction. Competition, predation, and proliferation are fundamental forces that drive ecological systems. Understanding how these forces come to shape basic food webs that contain some minimal numbers of species is no doubt a necessary step to unravel ecocomplexity.

It is well-known in theory that 1 prey/resource cannot support 2 competing predators/consumers at a stable equilibrium state ([12]). This is commonly refereed to as the Competitive Exclusion Principle (CEP). Like any simplistic generality from an overwhelmingly complex field, it has attracted a huge amount of attentions amongst experimental and theoretical ecologists and applied mathematicians. As with all general statements about ecological systems, field studies for CEP are inconclusive. Advances in the theory continued nevertheless. It was found in [1] and proved recently in [13] that such a system can have coexisting stable limit cycles. If one modifies the classical predator-prey systems for which CEP is based by tracking two essential elements, carbon and nitrogen, which are cycling through the species, then stable equilibrium coexisting states are indeed possible ([14]). Numerical evidence suggests that chaotic coexisting states are also possible for such stoichiometry mediated models ([15]). Coexistence also possible for chemostat population dynamics ([24]).

In this paper we will demonstrate that chaotic coexistence exists in the classical 2-to-1 predator-prey system when a top-predator is introduced to one of the competing predator. We will use a geometric method of singular perturbations which have proved to be extremely effective for ecological models, see [6, 7, 8, 13]. The idea is to recast the dimensional system so that the resulting dimensionless system is a singular perturbed one under the prolific diversification hypothesis ([6]) and that one-dimensional return maps can be constructed from the singular flows.

This work was funded in part by an NSF REU grant, #0139499, for the summer of 2002. B. Deng, G. Hines were the REU advisors. B. Bockelman, E. Green, L. Lippitt, and J. Sherman were the REU participants.

Chaos then follows when the one-dimensional return maps become unimodal or multimodal under appropriate conditions for the rescaled system.

The paper is organized as follows. In section 2 the basic model is introduced and scaled properly. Section 3 gives a brief review on singular perturbations and singular orbits, as well as some notation convention that will be used throughout the paper. In particular, we will review the technique of Pontryagin's delay of loss of stability in singular perturbations. In section 4 hypotheses and the main result are given, followed by a proof of the result in section 5. A few technical results are given the appendixes.

2. The Basic Model. To keep track of the 4 species interactions, let the population densities be X for the prey, Y, Z for the competing predators for the common prey X, and W for the top-predator on Y. We will assume that X is governed by Verhulst's logistic growth principle ([22, 16, 23]) in the absence of the predators, and all predators governed by Holling's Type II predation functional forms ([11]). These are 2 of the most fundamental modelling principles for ecological systems. Under the assumption that there are no other forms of competition between Y, Z, the dimensional model is as follows

$$(1)\qquad \begin{cases} \dfrac{dX}{dt} = rX\left(1-\dfrac{X}{K}\right) - \dfrac{p_1 X}{H_1+X}Y - \dfrac{p_2 X}{H_2+X}Z \\ \dfrac{dY}{dt} = \dfrac{b_1 p_1 X}{H_1+X}Y - d_1 Y - \dfrac{p_3 Y}{H_3+Y}W \\ \dfrac{dZ}{dt} = \dfrac{b_2 p_2 X}{H_2+X}Z - d_2 Z \\ \dfrac{dW}{dt} = \dfrac{b_3 p_3 Y}{H_3+Y}W - d_3 W \end{cases}$$

Here r is the intrinsic growth rate and K is the carrying capacity for the prey. Parameter p_1 is the maximal predation rate per predator Y and H_1 is the semi-saturation density for which when $X = H_1$ the Y's predation rate is half of its maximum, $p_1/2$. Parameter b_1 is predator Y's birth-to-consumption ratio and d_1 is its per-capita death rate. The remaining parameters have parallel and analogous meanings.

As a necessary first step for mathematical analysis, we non-dimensionalize Eq.(1) so that the scaled system contains a minimal number of parameters. It also has the advantage for uncovering equivalent dynamical behaviors with changes in different dimensional parameters. Using the same scaling ideas of [6] and the following specific substitutions for variables and parameters

$$(2)\qquad \begin{array}{l} t \to b_1 p_1 t, \quad x = \dfrac{X}{K}, \quad y = \dfrac{Y}{Y_0}, \quad z = \dfrac{Z}{Z_0}, \quad w = \dfrac{W}{W_0} \\ Y_0 = \dfrac{rK}{p_1}, \quad Z_0 = \dfrac{rK}{p_2}, \quad W_0 = \dfrac{b_1 p_1 Y_0}{p_3} \\ \zeta = \dfrac{b_1 p_1}{r}, \quad \epsilon_1 = \dfrac{b_2 p_2}{b_3 p_3}, \quad \epsilon_2 = \dfrac{b_3 p_3}{b_1 p_1} \\ \beta_1 = \dfrac{H_1}{K}, \quad \beta_2 = \dfrac{H_2}{K}, \quad \beta_3 = \dfrac{H_3}{Y_0} \\ \delta_1 = \dfrac{d_1}{b_1 p_1}, \quad \delta_2 = \dfrac{d_2}{b_2 p_2}, \quad \delta_3 = \dfrac{d_3}{b_3 p_3}, \end{array}$$

Eq.(1) is changed to this dimensionless form:

$$
(3) \qquad \begin{cases} \zeta \dfrac{dx}{dt} = x\left(1 - x - \dfrac{y}{\beta_1 + x} - \dfrac{z}{\beta_2 + x}\right) := xf(x,y,z) \\ \dfrac{dy}{dt} = y\left(\dfrac{x}{\beta_1 + x} - \dfrac{w}{\beta_3 + y} - \delta_1\right) := yg(x,y,w) \\ \dfrac{dz}{dt} = \epsilon_1 z\left(\dfrac{x}{\beta_2 + x} - \delta_2\right) := zh(x) \\ \dfrac{dw}{dt} = \epsilon_2 w\left(\dfrac{y}{\beta_3 + y} - \delta_3\right) := wk(y) \end{cases}
$$

The choice of these parameters can be explained as follows. The prey density X is scaled against its carrying capacity K, leaving x a dimensionless scalar. The predator is scaled against Y_0, which can be viewed as the predation capacity of the predator. The choice of Y_0 is motivated by the relation $p_1 Y_0 = rK$, i.e., the maximal rate of capture by Y_0 many Ys, $p_1 Y_0$, is equal to the capacity growth of the prey, rK. The scaling, $y = Y/Y_0$ thus gives y a scalar dimension. The scaling of the competitor Z is done similarly. The top-predator is scaled against it's predation capacity, W_0, at which $p_3 W_0 = b_1 p_1 Y_0$ with $b_1 p_1$ the maximal growth rate and Y_0 the Y-predation capacity.

The remaining parameters need to be explained a bit more as well. Parameters β_1, β_2, and β_3 are the ratios between the semi-saturation constants of the respective predators versus the carrying capacity of the respective preys. They are dimensionless semi-saturation constants in the scaled system (3). Parameters δ_1, δ_2, and δ_3 are relative death rates, each is the ratio of a predator's death rate to its maximal birth rate. As a necessary condition for species survival, the predator's death rate must be smaller than its maximal reproductive rate. Therefore we make a default assumption that $0 < \delta_i < 1$ for nontriviality.

The remaining parameters, $1/\zeta, \epsilon_1, \epsilon_2$, are the maximal growth rates of X, Z, W relative to Y, i.e., refereed to as the XY-prolificacy, ZY-prolificacy, and the WY-prolificacy respectively. By the theory of allometry ([3, 4]), these ratios correlate reciprocally well with the 4th roots of the ratios of X, Z, W's body masses to that of Y's. Thus they may be of order 1 when predator's and prey's body masses are comparable or of smaller order if, as in plankton-zooplankton-fish, and most plant-herbivore-carnivore chains, the body masses are progressively becoming heavier in magnitude so that ζ and ϵ_2 are small parameters. In any case, a given web will find its corresponding prolificacy characteristics in parameters ζ, ϵ_i which are now isolated in plain view in Eq.(3). The dimensional time t is recast to be $b_1 p_1 t$. In the new dimensionless time scale, $1(= b_1 p_1 t)$ unit equals $t = 1/(b_1 p_1)$ units in the original time scale, the average time interval between new births of Y.

3. Notation and Singular Perturbation Method. Consider the xy-subsystem of (3) in the absence of the competitor z ($z = 0$) and the top-predator w ($w = 0$):

$$
(4) \qquad \zeta \frac{dx}{dt} = x\left(1 - x - \frac{y}{\beta_1 + x}\right), \quad \frac{dy}{dt} = y\left(\frac{x}{\beta_1 + x} - \delta_1\right).
$$

It is singularly perturbed if $0 < \zeta \ll 1$. Variable y is the slow variable and the equation with $\zeta = 0$, $0 = xf(x,y,0)$ together with $dy/dt = yg(x,y,0)$, is the slow subsystem. It is a 1-dimensional equation on the slow manifold $x = 0$ and $0 = f(x,y,0)$, refereed to as the trivial and nontrivial x-nullcline respectively. Variable x is the fast variable and its equation with y frozen is the fast subsystem.

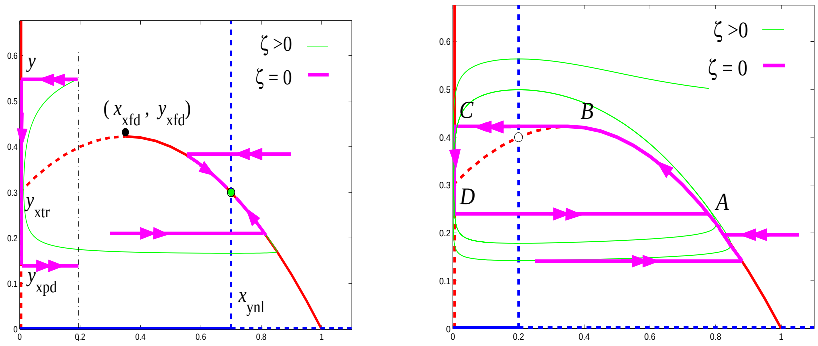

(a) (b)

Figure 1. (a) Typical singular orbits in the case of stable xy-equilibrium state for which $x_{\rm xfd} < x_{\rm ynl} < 1$. See text for the derivation of $y_{\rm xpd}$ for the phenomenon of Pontryagin's delay of loss of stability at which a population boom in x occurs although the recovery in x starts at y's crossing a greater y's density on the dashed threshold for the parabolic x-nullcline near $y_{\rm xtr}$. (b) A typical singular orbit in limit cycle and its relaxed cycle for $0 < \zeta \ll 1$ in the case $0 < x_{\rm ynl} < x_{\rm xfd}$.

More specifically, the fast subsystem is obtained by first rescaling the time $t/\zeta \to t$ to cast the system as $\dot x = xf(x,y,0)$, $\dot y = \zeta y g(x,y,0)$ and then setting $\zeta = 0$ to get $\dot x = xf(x,y,0), \dot y = 0$ for which y is frozen as a parameter. Fig.1(a,b) illustrate some of the singular orbits: horizontal phase lines are fast orbits and oriented curves on the x-capacity parabola and the extinction branch $x = 0$ are slow orbits. The directions of these orbits are determined by their corresponding directional fields. Typical fast orbits converge either to the predator-adjusted x-capacity on the parabola $f(x,y,0) = 0$, right of its fold point $(x_{\rm xfd}, y_{\rm xfd})$ with $f_x(x,y,0) < 0$ for attracting equilibrium points for the fast subsystem, or to the extinction branch $x = 0$ with $y > y_{\rm xtr}$. Typical slow orbits always move down on the depleted resource branch $x = 0$ and down or up on the capacity branch $f(x,y,0) = 0$ depending on whether the resource amount x is smaller or larger than $x_{\rm ynl}$, as in the y-nullcline $x = x_{\rm ynl}$, which is a required minimum to sustain the growth of the predator. The singular limit cycle in Fig.1(b) is the concatenation of fast and slow orbits with congruent orientation. We point out that the singular cycles and the equilibrium points will all persist for small $0 < \zeta \ll 1$ since their hyperbolicity can be verified and therefore the persistence results of [10, 2] can be applied. See [20, 19, 9, 21, 17, 5, 6, 13] for additional expositions on geometric methods of singular perturbations.

A few concepts will be used throughout the paper. Predator y is said to be *predatory efficient* if it can make the predator-induced prey capacity equilibrium $f(x,y,0) = 0$ to develop a crash fold point $x_{\rm xfd} = (1-\beta_1)/2 > 0$, namely $0 < H_1/K = \beta_1 < 1$. This means that the predator is able to reach half of its maximal predation rate at a prey density H_1 smaller than the prey's carrying capacity. Predator y is said to be *efficient* if it is predatory efficient and can actually crash the prey, that is, at the crash fold state $(x_{\rm xfd}, y_{\rm xfd})$ the predator can grow in per-capita:

$g(x_{\text{xfd}}, y_{\text{xfd}}, 0) > 0$, which is solved as $x_{\text{xfd}} = (1-\beta_1)/2 > \beta_1\delta_1/(1-\delta_1) = x_{\text{ynl}}$. It is easy to see that the relative mortality rate δ_1 should be small as part of the requirement for the predator to be efficient besides being predatory efficient. Predator y is said to be *weak* if it is not efficient.

A notation convention will be adopted throughout the paper. Presented by example, x_{xfd} means the x-coordinate of the fold point on the x-nullcline, and y_{xfd} is the y-coordinate of the same point. Thus x_{ynl} is the x-coordinate for the y-nullcline. Also, y_{xpd} is the y-coordinate of Pontryagin's delay of loss of stability point on the trivial x-nullcline, which we review below for the main analysis later. The exposition closely follows that of [20, 21].

Pontryagin's Delay of Loss of Stability: It deals with phenomena in which fast singular orbits jump away from the unstable trivial branch of the prey nullclines, in the asymptotic sense explained in the following paragraph. In practical terms, the predator declines in a dire situation of depleted prey $x = 0$, followed by a surge in the prey's recovery after the predator reaches a sufficient low density y_{xpd} to allow it to happen. The mathematical question is how the threshold y_{xpd} is determined.

Let $x = a$ with $0 < a < \min\{x_{\text{ynl}}, x_{\text{xfd}}\}$ be any line sufficiently near the y-axis. Let (a, y_1) be any initial point that is on the line and above the parabola. Let $(x_\zeta(t), y_\zeta(t))$ be the corresponding solution of the perturbed system (4) with $0 < \zeta \ll 1$ and with the initial point. The solution must move down because with $x = a$ less than the y-recovery minimum x_{ynl}, $\dot{y} < 0$. It moves leftwards above the unstable part of the parabola x-nullcline (where $f_x(x, y, 0) > 0$) until it crosses the parabola at a point $(x_p, y_p), 0 < x_p < a, \beta_1 = y_{\text{xtr}} < y_p$ at which the solution curve is vertical. It is near the transcritical point $(0, y_{\text{xtr}}) = (0, \beta_1)$ at which two branches of the x-nullcline, $x = 0$ and $f(x, y, 0) = 0$, intersect and the two branches exchange stabilities. The orbit then moves down but rightwards since now the x is in the recovery mode $\dot{x} > 0$. A finite time $T_\zeta > 0$ later it intersects the cross section line $x = a$ at a point denoted by $(a, y_2(\zeta))$. In general the second intercept $y_2(\zeta)$ depends on ζ. Now integrating along the solution curve we have

$$\begin{aligned} 0 = \zeta \ln x|_a^a &= \int_0^{T_\zeta} \frac{\zeta \dot{x}_\zeta}{x_\zeta} dt = \int_{y_1}^{y_2(\zeta)} \frac{\zeta \dot{x}_\zeta}{x_\zeta \dot{y}_\zeta} dy_\zeta \\ &= \int_{y_1}^{y_2(\zeta)} \frac{f(x_\zeta, y_\zeta)}{y_\zeta g(x_\zeta, y_\zeta)} dy_\zeta. \end{aligned}$$

Taking limit $\zeta \to 0$ on both sides of the equation above, using the facts that $x_\zeta \to 0, x_p \to 0, y_p \to y_{\text{xtr}} = \beta_1$ and the notations that $y_1 = y, y_2(\zeta) \to y_{\text{xpd}}, y_\zeta \to s$, we obtain the integral equation

$$\int_{y_{\text{xpd}}}^{y} \frac{f(0, s, 0)}{s g(0, s, 0)} ds = 0$$

for variables y and y_{xpd}. In practical terms, y approximates the value followed by a collapse in x starting at the initial (a, y) and y_{xpd} approximates the value that immediately precedes an outbreak in x. Because the integrant $f(0, s, 0)/sg(0, s, 0)$ has opposite signs for $s > y_{\text{xtr}}$ and for $s < y_{\text{xtr}}$, we immediately conclude the following qualitative property: the greater concentration y at the onset of x's collapse the lower concentration y_{xpd} it reaches before the x-outbreak can take place. We also have its quantification: y_{xpd} is the value so that the two areas bounded by the integrant graph are equal: $\int_{y_{\rm xtr}}^{y} \frac{f(0,s,0)}{sg(0,s,0)}ds = \int_{y_{\rm xpd}}^{y_{\rm xtr}} -\frac{f(0,s,0)}{sg(0,s,0)}ds$. Notice that the branch $\{x = 0, y < y_{\rm xtr}\}$ is effectively unstable for the fast x-subsystem.

The above phenomenon that singular orbits develop beyond a transcritical point, continue along the unstable part of a nullcline before jumping away is called *Pontryagin's delay of loss of stability*. The case illustrated is for the type of transcritical points at which the fast variable goes through a phase of crash-recovery-outbreak. In other cases of generalization, they may be responsible for a reversal phase for the fast variable. However, all the known PDLS cases of our $XYZW$-model are of the crash-recovery-outbreak type described above. We often call them outbreak PDLS points.

4. Conditions and The Main Result. We now set up the parameter regions for which the type of chaotic dynamics that we consider for this paper arises. We will do so by listing a series of conditions for which the equations are assumed to satisfied.

Condition 1. *The chain prolific diversification condition: the maximal per-capita growth rates decrease from the bottom to the top along a food chain, and the differences between the rates are drastic:*

$$0 \ll b_3p_3 \ll b_1p_1 \ll r, \text{ equivalently, } 0 < \epsilon_2 \ll 1 \ll \frac{1}{\zeta}.$$

We note that this condition was referred to as 'the trophic time diversification hypothesis' in [18, 6]. For the ZY-prolificacy parameter ϵ_1, it is not obvious that the prolificacy hypothesis should or should not apply since Y, Z are competitors rather than chain predators. It may range from very small to very large. We will assume

Condition 2. *Predator Z reproduces faster than W but slower than Y:*

$$0 \ll b_3p_3 \ll b_2p_2 \ll b_1p_1 \ll r, \text{ equivalently, } 0 < \epsilon_2 \ll \epsilon_1 \ll 1 \ll \frac{1}{\zeta}. \tag{5}$$

One definitive mathematical advantage stemming from these assumptions is obvious: it allows us to treat the system as a singular perturbed system for which a whole array of tools are available both geometrical and analytical.

Next we introduce 2 more conditions which are related to the xyz competing predators and prey system with $w = 0$:

$$\zeta\frac{dx}{dt} = xf(x, y, z),\ \frac{dy}{dt} = yg(x, y, 0),\ \frac{dz}{dt} = \epsilon_1 zh(x),$$

and the exclusion of stable xyz-equilibrium point.

Since both predators' nontrivial nullclines are parallel planes: $g(x, y, 0) = 0, h(x) = 0$ giving rise to

$$x = x_{\rm ynl} = \beta_1\delta_1/(1 - \delta_1), \quad x = x_{\rm znl} = \beta_2\delta_2/(1 - \delta_2), \tag{6}$$

respectively, we conclude right away that there does not exist coexisting xyz-equilibrium state if $x_{\rm ynl} \neq x_{\rm znl}$ which is typically expected. We will limit our attention to the case where in the absence of y the xz-equilibrium point is stable, and similarly in the absence of z the xy-equilibrium point is stable. The first condition we want requires a further restriction below.

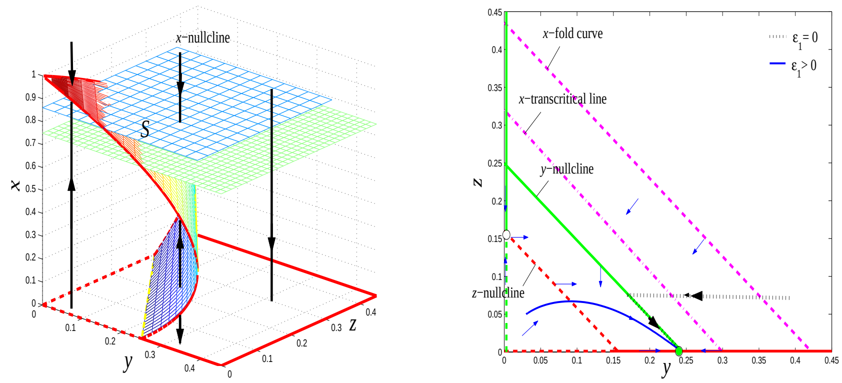

(a) (b)

FIGURE 2. (a) A 3-d view of the nullcline surfaces is shown. The stable branches of the x-nullcline are outlined in solid bold and unstable branches by dashed bold. Vertical phase lines are x-fast flows. The parallel planes are the nontrivial y-nullcline and z-nullcline surfaces both of which lie above the x-fold curve since y, z are jointly weak. (b) A reduced 2-d phase portrait view. A case of non-competitive z is shown. Solid vector field and solution curves are for a perturbed case $\epsilon_1 > 0$ and dotted curves are singular orbits at the singular limit $\epsilon_1 = 0$. Both lead to the z-extinction scenario.

For the singularly perturbed xyz-system, the attracting, nontrivial, slow manifold is part of the x-nullcline surface $f(x, y, z) = 0$ for which $f_x(x, y, z) < 0$. It consists of yz-adjusted carrying capacity for the prey. Points on the surface must have the property that the x value must decrease with any increase in either y or z or both. We denote this surface $\mathcal{S}$ and its projection onto the yz-plane D for later usage. Similar to the 1-dimensional crash fold point $(x_{\rm xfd}, y_{\rm xfd})$, a joint crash fold point developed at a given pair of (y, z) if at (y, z) there is an adjusted capacity x which disappears upon any small increase either in y or z. The set of these crash fold points is a curve whose y-coordinate and z-coordinate are reciprocal in relation: increasing the z-predation pressure only requires a smaller amount of predator y to crash the prey, and vice versa. Denote the fold crash points similarly by $(x_{\rm xfd}, y_{\rm xfd}, z_{\rm xfd})$. It is part of the boundary of the capacity surface $\mathcal{S}$ and determined analytically by $f(x, y, z) = 0, f_x(x, y, z) = 0$.

Condition 3. *The joint yz-weak condition: The y-nullcline plane $x = x_{\rm ynl}$ lies above the crash fold curve $(x_{\rm xfd}, y_{\rm xfd}, z_{\rm xfd})$ and analogously the z-nullcline plane $x = x_{\rm znl}$ lies above the crash fold curve as well.*

Recall that y is weak if $x_{\rm ynl}|_{\{z=0\}} > x_{\rm xfd}|_{\{z=0\}}$ and z is weak if $x_{\rm znl}|_{\{y=0\}} > x_{\rm xfd}|_{\{y=0\}}$. Thus the joint yz-weak condition implies individual weakness but the converse is not necessarily true.

Joint weakness implies that everywhere along the crash fold curve, none of the predators can grow. In other words, once a ζ-slow singular orbit starts on the predator-adjusted carrying capacity $\mathcal{S}$, the orbit will stay on the surface because along the crash fold, a boundary of $\mathcal{S}$, the vector fields point into the capacity surface. Moreover if a singular orbit is not on $\mathcal{S}$, it will eventually be attracted to and stay on $\mathcal{S}$. This is because if it is attracted to the only other alternative trivial x-nullcline $x = 0$, then the dynamics will force y, z to decrease and eventually cross the x rebound/outbreak transcritical line (see Fig.2) and jump onto the x-capacity branch, guaranteed by the principle of Pontryagin's delay of loss of stability. Therefore we can conclude the following:

Proposition 1. *Under the joint yz-weak condition the predator-adjusted prey capacity manifold $\mathcal{S} : f(x, y, z) = 0, f_x(x, y, z) < 0$ attracts all singular orbits and it is invariant for the yz-slow subsystem.*

The joint yz-weakness condition can be expressed explicitly as follows

$$\min\{x_{\text{ynl}}, x_{\text{znl}}\} = \min_{i=1,2}\{\frac{\beta_i\delta_i}{1-\delta_i}\} > \max_{i=1,2}\{\frac{1-\beta_i}{2}\} = \max\{x_{\text{xfd}}|_{\{y=0\},\{z=0\}}\}. \tag{7}$$

The derivation is given in Appendix A.

The next condition is about the relative competitive edge between y, z. Because of its invariance, the ζ-slow subdynamics on $\mathcal{S}$ is only 2-dimensional and we can take the advantage by conducting our analysis on the surface or equivalently on the projected yz-plane region D, as shown in Fig.2. It is easier to make sense of the vector field plot by keeping in mind that if y, z are closer to the origin then the prey supply x is closer to its capacity 1 because they are confined to the capacity manifold $\mathcal{S}$. Therefore on the project vector field in the yz-plane, both y, z increase near the origin. More precisely, if y is below its nullcline, its food supply is relatively abundant and y increases. For y above its nullcline, it decreases. Similar conclusions apply to z.

Condition 4. *Species z is not competitive against species y, that is the xy-equilibrium point is attracting in the z-direction, i.e. $h(x_{\text{ynl}}) < 0$ which solves as:*

$$x_{\text{znl}} = \frac{\beta_2\delta_2}{1-\delta_2} > \frac{\beta_1\delta_1}{1-\delta_1} = x_{\text{ynl}}.$$

In practical terms, y can manage to increase its population in the interim prey supply $x_{\text{ynl}} < x < x_{\text{znl}}$ which on the other hand is not enough to support z's rebound since predator's nullcline value represents the minimal threshold amount in prey supply to sustain that predator's population growth. In terms of the ζ-slow dynamics on the capacity surface $\mathcal{S}$ and equivalently in the projected region D, the y-nullcline and z-nullcline do not intersect, and the less competitive species nullcline is closer to the origin than the competitive ones. A straightforward phase plane analysis leads to the conclusion that the noncompetitive species goes to extinction. To summarize, we have

Proposition 2. *Under the joint yz-weak condition and the condition that z is noncompetitive against y, all singular orbits converge to the xy-fixed point with $z = 0$.*

The last condition we impose concerns the xyw food chain with $z = 0$:

$$\zeta\frac{dx}{dt} = xf(x, y, 0),\ \frac{dy}{dt} = yg(x, y, w),\ \frac{dw}{dt} = \epsilon_2 wk(y),$$

and the exclusion of stable xyw-equilibrium points.

Condition 5. *Species W is efficient.*

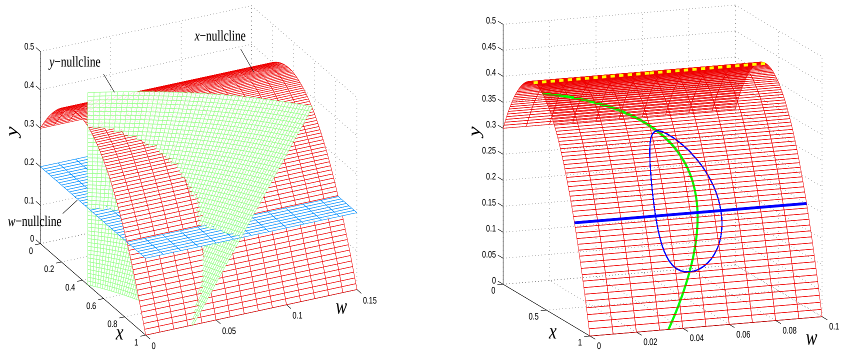

(a) (b)

FIGURE 3. (a) A sample of computer generated x, y, w nullclines in the xyw-space. (b) An xyw-slow cycle as y is weak and w is efficient. Parameters values: $\zeta = 0.1, \epsilon_1 = 0.1, \epsilon_2 = 0.1, \beta_1 = 0.3, \beta_2 = 0.57, \beta_3 = 0.2, \delta_1 = 0.6, \delta_2 = 0.54, \delta_3 = 0.5$, and $z = 0$.

This means that the ζ-slow, yw-dynamics on the x-slow manifold $\mathcal{S} \cap \{z = 0\}$ is a 2-species predator-prey system for which the y-nullcline develops a crash fold point at which the predator w is able to crash it. Qualitatively speaking this requires both β_3, δ_3 to be relatively small. This description can be made in more analytical details below.

The nontrivial x-slow manifold is a parabola cylinder parallel to the w-axis:

$$y = (1 - x)(\beta_1 + x), \text{ for } 0 \leq x \leq 1.$$

It is the same x-nullcline as for the xy-system extended in the positive w-axis direction. All the properties about the x-nullcline can be directly borrowed from preceding analyses. Its fold line is $(x, y) = (x_{\rm xfd}, y_{\rm xfd}) = ((1-\beta_1)/2, (1+\beta_1)^2/4)$ and the attracting branches of the x-slow manifold are $\mathcal{S} \cap \{z = 0\}$, which is the parabola between $x_{\rm xfd} < x < 1$, and the trivial manifold $x = 0$ above the transcritical line $y > y_{\rm xtr} = \beta_1$. The constraint y-nullcline on $\mathcal{S} \cap \{z = 0\}$ consists of the w-adjusted xy capacity/equilibrium state. Denote it by $\gamma = \{g = 0\} \cap \{f(x, y, 0) = 0\}$. Qualitatively, this w-adjusted xy-capacity must decrease in y with increase in w, further moving away from the x crash fold on the x-capacity surface. Since y is weak, the capacity curve γ lies below the fold density $y_{\rm yfd}$ when $w = 0$ and hence lies below it entirely. Therefore the x-capacity surface $\mathcal{S} \cap \{z = 0\}$ is globally attracting and invariant with respect to the ζ-slow yw-dynamics. The reduced dynamics is again singularly perturbed by ϵ_3, and as a consequence the same analysis for the predator-prey xy-system applies, with only some minor modifications to be made for y, w on the surface $\mathcal{S} \cap \{z = 0\}$.

As with the planar case, the singular ζ-slow dynamics on $\mathcal{S} \cap \{z = 0\}$ is determined by the configurations of the y-nullcline γ and the w-nullcline, $y = y_{\rm wnl} = \beta_3\delta_3/(1-\delta_3)$ with $k(y_{\rm wnl}) = 0$. Recall that the top-predator w is predatory efficient if it can cause the xy-capacity/equilibrium curve γ to develop a crash fold point. As a special case of Proposition 5 with $z = 0$ from Appendix B, it occurs under the following condition

$$\beta_3 < \frac{(\beta_1+1)^3}{\beta_1}\left(\frac{1}{\beta_1+1} - \delta_1\right) \tag{8}$$

and the crash fold point is unique. Notice that the y-crash fold develops only when β_3 is relatively small, the predatory efficiency requirement on the part of w. Like the planar xy-subsystem case, it separates γ into two parts: the top part contains the w-adjusted xy-capacity equilibria, which is y-stable, and the bottom part, which is y-unstable. The intersection with the trivial branch $\{y = 0, x = 1\}$ at $y = 0, w_{\rm ytr} = \gamma(1)$ is the only y-rebound/outbreak transcritical point at which PDLS phenomenon also occurs. Unlike the planar case, the fold point $(x_{\rm yfd}, y_{\rm yfd}, w_{\rm yfd})$ cannot be explicitly expressed. Nevertheless, it is well-defined that w is efficient iff $y_{\rm wnl} < y_{\rm yfd}$, where $y = y_{\rm wnl}$ defines the w-nullcline $k(y_{\rm wnl}) = 0$. That is, w increases at the fold $k(y_{\rm yfd}) > 0$ and therefore it will crash its prey. As a result from the same arguments as in the planar case there exits a singular limit cycle on the x-capacity surface $\mathcal{S} \cap \{z = 0\}$, see Fig.3.

The last condition is about the w-induced z-competitiveness.

Condition 6. *Species Z is competitive in the $XYZW$-web, which means the xyw-cycle is repelling in the z-direction, that is the per-capita growth rate for z averaged along the cycle is positive:*

$$J = \int_0^{T_c} h(x_c(s))ds > 0,$$

where $(x_c, y_c, 0, w_c)(t)$ denotes the cycle and T_c the period.

Now we are ready to state the main result of this paper.

Theorem 1. *The dynamics of Eq.3 can be chaotic in the sense of having a subdynamics equivalent to shift dynamics on 2 symbols if conditions 1, 2, 3, 4, 5, and 6 are satisfied.*

To summarize the conditions of the theorem analytically, we have

$$x_{\rm ynl} = \frac{\beta_1\delta_1}{1-\delta_1} > \max_{i=1,2}\{\frac{1-\beta_i}{2}\} = \max\{x_{\rm xfd}|_{\{y=0\}}, x_{\rm xfd}|_{\{z=0\}}\}$$

which is the combination of Condition 3, equivalently (7), and Condition 4; the w predatory efficient condition (8) and the w-efficient condition $y_{\rm wnl} = \beta_3\delta_3/(1-\delta_3) < y_{\rm yfd}$ with $y_{\rm yfd}$ defined from Proposition 5; and the prolificacy conditions (5). As an example, a set of parameter values from these regions is found to give rise to the type of chaotic attractors stated in the theorem. See Fig.4. The remainder exposition is to demonstrate how such structures emerge and why shift maps or 1-dimensional unimodal or multimodal maps capture their dynamics.

5. Proof of The Main Result. We now consider the full $xyzw$-web equations (3). We will mostly use holistic and geometrical arguments and leave some nonessential technicalities to Appendix C.

Dimension Reduction. The nontrivial x-nullcline $f(x, y, z) = 0$, its crash-fold, stable, and unstable branches are the same for the full system as for its xyz-subsystem because w does not directly interact with x. We use the same notation $\mathcal{S}$ as in the previous sections for the stable branch of the nontrivial x-nullcline. It is the same as before except that it is a 3-dimensional solid in the $xyzw$-space.

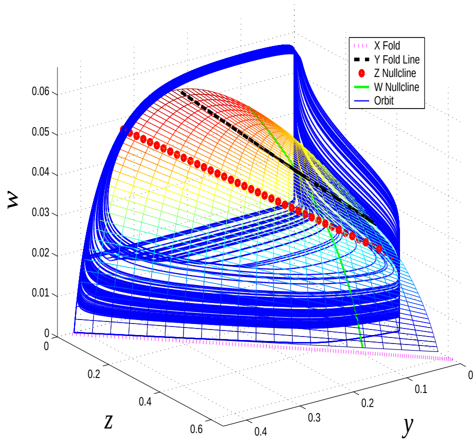

(a)

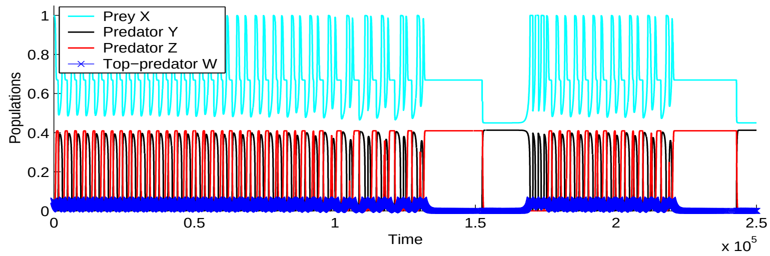

(b)

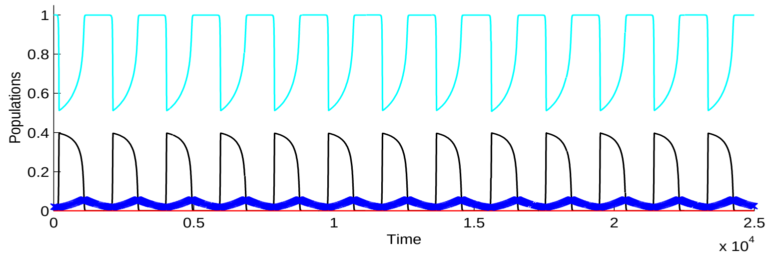

(c)

FIGURE 4. With parameter values $\zeta = 0.1, \epsilon_1 = 0.1, \epsilon_2 = 0.004, \beta_1 = 0.3, \beta_2 = 0.57, \beta_3 = 0.2, \delta_1 = 0.6, \delta_2 = 0.54, \delta_3 = 0.3$, the dynamics is a rather wild chaotic attractor, showing both in (a) the yzw-projected view and in (b) the time series. Without the z-species ($z = 0$), the dynamics is an xyw limit cycle as shown in (c) because w is efficient.

As demonstrated earlier, because of the joint yz-weak assumption, both y, z are in a decline mode near the x-fold state, hence preventing x from crashing, which in turn implies that the surface $\mathcal{S} \cap \{w = 0\}$ is invariant for the ζ-slow yz-subsystem. With the presence of w predation, y must be in a steeper decline near the x-fold than without, and for the same reason crashing in x is impossible and more so. Hence the solid $\mathcal{S}$ is invariant for the full ζ-slow yzw-system.

Any point (x, y, z, w) from the solid $\mathcal{S}$ can be expressed as a function of y, z, $x = q(y, z)$. It means for each level of y, z predation, there is a unique yz-adjusted carrying capacity of the prey, which by definition defines the stable nontrivial branch of the x-nullclline. Also, the function q is decreasing in both y and z because any elevated predatory pressure depresses the adjusted prey steady state further.

On the trivial x-slow manifold $x = 0$, the transcritical points for the full web remain the same as for the xyz-web. All ζ-singular orbits must cross it and jump to the solid $\mathcal{S}$ at some x-outbreak PDLS points for the reason that x and w do not directly interact with each other. Therefore, all nontrivial ζ-singular orbits eventually settle down into the invariant solid $\mathcal{S}$. And we only need to consider the 3-dimensional yzw-slow system in $\mathcal{S}$. A dimension reduction is now obtained.

Mathematically, S is defined by $f(x, y, z) = 0, f_x(x, y, z) < 0$. Because of the hyperbolicity $f_x(x, y, z) < 0$, variable x can be solved by the Implicity Function Theorem as a function $q(y, z)$ from $f(x, y, z) = 0$ with (y, z) from the same set D that is bounded by the y, z axis and the x-fold boundary of $\mathcal{S}$ projected onto the yz-plane. Also q is a decreasing function in both y and z: $q_y(y, z) < 0, q_z(y, z) < 0$ (see Appendix C). The ζ-slow yzw-system in $\mathcal{S}$ is then expressed explicitly as follows:

$$(9) \qquad \begin{cases} \dfrac{dy}{dt} = y\left(\dfrac{q(y,z)}{\beta_1 + q(y,z)} - \dfrac{w}{\beta_3 + y} - \delta_1\right) = yg(q(y,z), y, w) \\ \dfrac{dz}{dt} = \epsilon_1 z\left(\dfrac{q(y,z)}{\beta_2 + q(y,z)} - \delta_2\right) = zh(q(y,z)) \\ \dfrac{dw}{dt} = \epsilon_2 w\left(\dfrac{y}{\beta_3 + y} - \delta_3\right) = wk(y) \end{cases}$$

Qualitative Properties of Nullcline Surfaces. We begin our singular orbit analysis in $\mathcal{S}$ by first describing the y, z, w nullclines holistically and geometrically. The technicalities are left to Appendixes B,C.

The nontrivial w nullcline for the reduced system (9) is the simplest: $k(y) = 0 \Longrightarrow y = y_{\text{wnl}} = \beta_3\delta_3/(1 - \delta_3)$, a plane parallel to the zw-plane in $\mathcal{S}$. On this plane either recovery or decline in w takes place depending on whether or not its prey y is in creasing or decreasing mode. To the side $y < y_{\text{wnl}}$, w decreases because of insufficient food supply. Otherwise, w increases if $y > y_{\text{wnl}}$.

The nontrivial z nullcline is slightly more complicated: $h(q(y, z)) = 0 \Longrightarrow q(y, z) = x_{\text{znl}} = \beta_2\delta_2/(1 - \delta_2)$ because of (6). It is a surface parallel to the w-axis, through a curve $q(y, z) = x_{\text{znl}}$ on the yz-plane. It is the same z-nullcline when the conditions of joint yz-weakness and z-noncompetitiveness were introduced. It defines the y competition-adjusted xz equilibrium state. When setting y in a dynamical motion, it is also the state where z either rebounds from a decline or declines from a growth depending on whether or not the competition strength from y weakens ($\dot{y} < 0$) or intensifies ($\dot{y} > 0$). We already know the function q decreases in both y and z. Hence to maintain a constant level $q(y, z) = x_{\text{znl}}$, y and z must behave in opposite manners on the curve: increasing y must be counter-balanced by decreasing z. Therefore, the curve has negative slopes everywhere in $\mathcal{S}$.

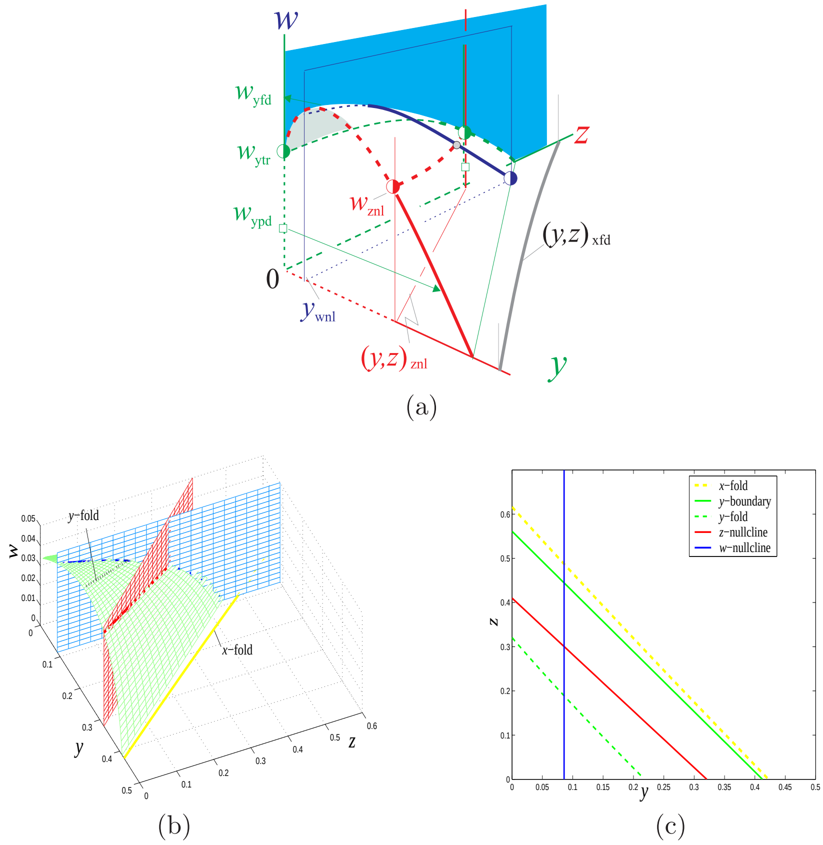

FIGURE 5. (a) A sketch based on the qualitative descriptions on the nullcline surfaces inside the x-nullcline solid $\mathcal{S}$. The stable branch of the trivial y-nullcline is shaded. The unstable branch of the nontrivial y-nullcline surface $w = q(y, z)$ lies between the y crash-fold $(y_{\rm yfd}, z_{\rm yfd}, w_{\rm yfd})$ and the transcritical curve $(0, z_{\rm ytr}, w_{\rm ytr})$. Vertical planes are the nontrivial w and z nullcline surfaces respectively. Their intersections with the stable nontrivial y-nullcline surface $w = q(y, z)$ are the solid and dashed curves respectively. (b) Numerically generated nullcline surfaces. The solid $\mathcal{S}$ is bounded by the x-fold plane parallel to the w-axis. (c) The same surfaces of (b) in the yz-projected view. Left to the y-fold curve, the y-nullcline surface is unstable, and to its right, it is stable. The y-nullcline surface is bounded by the coordinate axes and the dotted y-boundary curve.

The most complex nullcline is the y-nullcline surface: $g(q(x, y), y, w) = 0$, which, by solving for w, is expressed as

$$w := p(y, z) = \left(\frac{q(y, z)}{\beta_1 + q(y, z)} - \delta_1 \right) (\beta_3 + y). \tag{10}$$

As with other nullclines, this surface is the w-predation and z-competition adjusted capacity or threshold states for y. In a dynamical motion, they defines the states at which the predator y either recovers from a fall or declines from a rise depending on the strength of z-competition and w-predation. If z-competition is strong ($\dot{z} > 0$) or the w-predation is repressive ($\dot{w} > 0$), then y falls from growing to decline at the state. Otherwise it turns from decline to recovery.

Two special cases are already known: the case with $w = 0$ from the analysis of the xyz-web and the case with $z = 0$ from the analysis of the xyw-chain. In what follows we continue on a practical description of the surface and more importantly its intersections with the other two nullcline surfaces.

The range in y, z over which the surface $w = p(y, z)$ is positive is precisely the delta shaped region bounded by the y, z axes and the y-nullcline curve $g(q(y, z), y, 0) = 0$, i.e. $q(y, z) = x_{\rm ynl}$ from (6). From the expression of (10) for $w = p(y, z)$ above, we see that $p(y, z) > 0$ if and only if $q(y, z)/(\beta_1 + q(y, z)) - \delta_1 > 0$ which in turn solves as $q(y, z) > \beta_1\delta_1/(1 - \delta_1) = x_{\rm ynl}$. Since we already know q is decreasing in both y and z, so for this inequality to hold, y and z must be smaller yet than they would be at the equality $q(y, z) = x_{\rm ynl}$. Hence the domain is given as

$$\Delta := \{ \text{ the first quadrant left of the } y\text{-nullcline curve } q(y, z) = x_{\rm ynl} \text{ on } w = 0\}$$

Alternatively, for a fixed competition intensity of z, and an elevated predatory pressure $w > 0$, the adjusted equilibrium y level must be lower than what would be if the top-predation is absent, $w = 0$. Either way, we know the surface in $\mathcal{S}$ lies above the delta-shaped region Δ.

The topography of the surface can be understood holistically as well. From the expression $w = p(y, z) = (q(y, z)/(\beta_1 + q(y, z)) - \delta_1)(\beta_3 + y)$ we can readily see from a domino effect that if y is fixed, increasing z decreases the steady x supply $x = q(y, z)$ in $\mathcal{S}$, which in turn decreases the quantity $q(y, z)/(\beta_1 + q(y, z))$, which represents the per-capita catch $x/(\beta_1 + x)$ by y, and hence decreases the p-value. In practical terms, if y is fixed and the z competition level is increased, then it only requires a smaller w amount of predatory pressure to separate the waxing phase $\dot{y} > 0$ from the waning phase $\dot{y} < 0$ of y. Looking at it either ways, the y-section curves on the surface are all decreasing in z, all the way down to $w = 0$ on the boundary of Δ.

It is slightly more complex to visualize the z-section curves on the surface. Begin with the special case $z = 0$, we know that the y-nullcline can have a y-crash-fold from the analysis of efficient w condition. It separates the y-nullcline into the w-adjusted capacity state and the y-threshold state. The former is stable and the latter is unstable for the y-dynamics. The stable branch is a monotone decreasing function of w: fixed at a greater w depletes the steady supply y. The unstable, threshold branch is a monotone increasing function of w: fixed at a greater w requires a greater threshold amount of y for y to increase. The two branches coalesce at the crash fold.

Now fix z at an increased value $z > 0$, the competition makes fewer resource available for y, and makes y more vulnerable. Hence it takes a smaller w amount to crash y. In other words, intensified z competition drives down y in capacity, therefore increases the relative semi-saturation density (= [Semisaturation]/[Y Capacity]) for w which in turn amounts to making w weaker as a predator. Since the w-nullcline, $y = y_{\rm wnl} = \beta_3\delta_3/(1 - \delta_3)$, contains parameter δ_3 which is independent of the parameters that defines the y nullcine surface, we can use it to sweep the surface

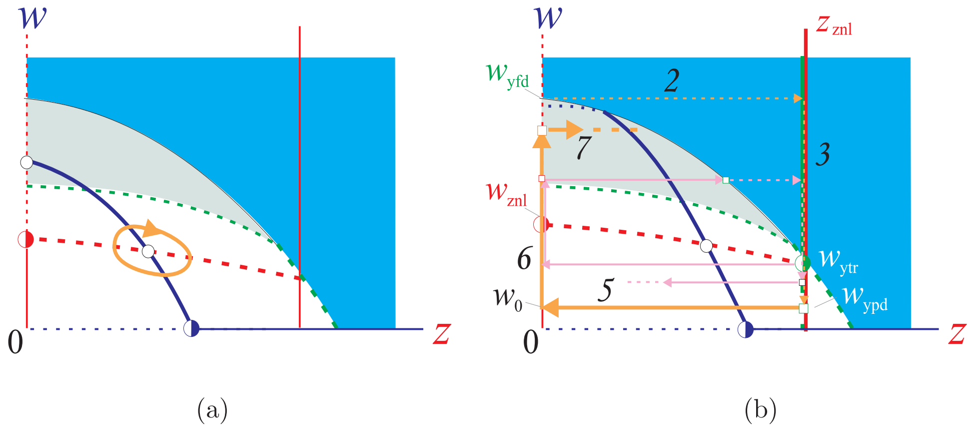

FIGURE 6. (a) A y-slow cycle born through Hopf bifurcation at $\mathcal{E}$. (b) It grows into a large singular cycle showing the case of w-nullcline going through the y-fold. In the case of (a) and as $\epsilon_2/\epsilon_1 \to 0$, the cycle grows but will never surpass the level $w = w_{\rm wnl}$, at which the xyw-equilibrium point shown is not stable.

to determine the structure of the crash-fold. Now if $y = y_{\rm wnl}$ is exactly at the crash-fold $y_{\rm yfd}$ for a given z and a chosen δ_3, then for a larger z, the corresponding yw-dynamics should be weaker in w. Since the w-nullcine $y = y_{\rm wnl}$ remains the same, then for w to be weak the y-crash point must drop lower than $y_{\rm wnl}$ so that w cannot dynamically crash it. What about the crash density $w_{\rm yfd}$? Since increasing z decreases w along the surface, the corresponding crash density $w_{\rm yfd}$ is smaller than the w value for the original z at the smaller crash density $y_{\rm yfd}$. Since the crash density $w_{\rm yfd}$ at the original z is the largest w value along the z-section, the crash density $w_{\rm yfd}$ for the larger z must be smaller than that for the original smaller z. Hence, we can conclude that the y-crash-fold decreases not only in the w-coordinate $w_{\rm yfd}$ but also in the y-coordinate $y_{\rm yfd}$ when z is increased.

Finally, it is left to describe the intersections of these nullcline surfaces. The intersection of the w-nullcline surface $y = y_{\rm wnl}$ with the y-nullcline $x = p(y, z)$ is a monotone decreasing curve of w in z as we have already derived this property for all y-section curves on the surface $w = p(y, z)$. The intersection of the z-nullcline $x = q(y, z) = x_{\rm znl}$ with the y-nullcline surface is $w = p(y, z) = (x_{\rm znl}/(\beta_1 + x_{\rm znl}) - \delta_1)(\beta_3 + y)$ which is, obviously, a monotone increasing line in y. In practical terms, increasing y decreases z on the fixed supply level $x = x_{\rm znl}$ of x. This improves the status of predator y. As a result, it would take a greater amount of the top-predator w to flip a growing y mold $\dot{y} > 0$ to a declining mold $\dot{y} < 0$. With the constant supply $x = q(y, z) = x_{\rm znl}$, increasing z decreases y, which in turn decreases $w = p(y, z) = (x_{\rm znl}/(\beta_1 + x_{\rm znl}) - \delta_1)(\beta_3 + y)$. So the intersection curve is a decreasing function of w as z increases.

All the descriptions above are incorporated into the illustration of Fig.5. The analytical justification is given in Appendix C.

Singular Cycle. We start the analysis by constructing a cycle as a precursor to the chaotic attractor. The cycle has smaller variation in w than y and z. First we describe the key conditions that will allow us to trap such an orbit. Start at the y-fold point $(y_{\rm yfd}, 0, w_{\rm yfd})$ on $z = 0$, c.f. Fig.6(b). Following the y-fast flow, the singular orbit (orbit 1) lands on the trivial y-nullcline surface $y = 0$ with the other coordinates unchanged. Then the z-fast dynamics takes over, sending the orbit (orbit 2) horizontally to the attracting z-nullcline $y = 0, z = z_{\rm znl}$, landing on it with the same w-coordinate $w_{\rm yfd}$. See both Figs.6(b),7(a). Once on the line $y = 0, z = z_{\rm znl}$, the w-dynamics takes over, and the slow w-orbit (orbit 3) develops downwards. It first crosses the y-transcritical point $(y, z, w) = (0, z_{\rm znl}, w_{\rm ytr})$, and must then jump to the nontrivial y-slow manifold $w = p(y, z)$ at a y-PDLS point $(0, z_{\rm znl}, w_{\rm ypd})$ due to Pontryagin's delay of loss of stability with respect to the fast y-flow (orbit 4). The value of $w_0 := w_{\rm ypd}|_{\{z=z_{\rm znl}\}}$ is determined as follows.

First we need to be more specific about the time scales of the reduced yzw-system in the solid $\mathcal{S}$. Rescale the time $t \to \epsilon_2 t$ to obtain the reduced system as

$$\epsilon_2 y' = yg(q(y, z), y, w),\ \epsilon_0 z' = zh(q(y, z)),\ w' = wk(y)$$

with $\epsilon_0 = \epsilon_2/\epsilon_1 \ll 1$ as an independent singular parameter from ϵ_2. Thus, under the condition that $0 < \epsilon_2 \ll \epsilon_1 \ll 1$, y is the fastest of the three at a rate of order $O(1/\epsilon_2)$, z is the second fastest at a rate of order $O(1/\epsilon_0) = O(\epsilon_1/\epsilon_2) \ll O(1/\epsilon_2)$.

Take any plane $y = y_0 > 0$ sufficient near $y = 0$. Then a perturbed orbit starting from $(y_0, z_0, w_{\rm yfd})$ for $z_0 > 0$ is first attracted to the trivial y-nullcline $y = 0$ (similar to orbit 1), only to emerge somewhere below the y-slow manifold $w = p(y, z)$ and move toward the manifold (similar to orbit 4). In doing so it will hit the plane $y = y_0$ again in direction opposite to its initial direction. Hence following the orbit, the integral identity below holds

$$0 = \int_{y_0}^{y_0} \frac{1}{\epsilon_2 y} dy.$$

Since we can choose $0 < y_0 < y_{\rm wnl}$, the w-component of this portion of the orbit always decreasing in w. Thus, we can make the following substitution of variable from y to w

$$0 = \int_{y_0}^{y_0} \frac{1}{\epsilon_2 y} dy = \int_{w_{\rm yfd}}^{w_{\rm ypd}} \frac{1}{\epsilon_2 y} \frac{dy}{dw} dw.$$

Simplify the integral to obtain

$$0 = \int_{w_{\rm yfd}}^{w_{\rm ypd}} \frac{g(q(y, z), y, w)}{wk(y)} dw.$$

Taking the limit $\epsilon_2 \to 0$ first, we have $y = 0$ on the equation above since $dw = 0$ on orbit 1 and orbit 4. Taking the limit $\epsilon_0 \to 0$ next for the reduced zw-system, we have $z = z_{\rm znl}$ for z of the integrant since $dw = 0$ on orbit 2. Therefore at the limit $\lim_{\epsilon_0 \to 0} \lim_{\epsilon_2 \to 0}$, the integral equation above becomes

$$0 = \int_{w_{\rm yfd}}^{w_{\rm ypd}} \frac{g(q(0, z_{\rm znl}), 0, w)}{wk(0)} dw,$$

defining the $w_{\rm ypd}$ value on $z = z_{\rm znl}$ as shown in Fig.6(b) as well as 7(a). Because $g(q(0, z_{\rm znl}), 0, w) < 0$ for $w > w_{\rm ytr}$ and $g(q(0, z_{\rm znl}), 0, w) > 0$ for $0 < w < w_{\rm ytr}$, and the fact that the indefinite integral

$$\int_{w_{\rm ytr}}^{u} \frac{g(q(0, z_{\rm znl}), 0, w)}{wk(0)} dw$$

is 0 at $u = w_{\rm ytr}$ and $+\infty$ at $u = 0$, the integral equation above for the y-PDLS point $w_{\rm ypd}$ has a unique solution between 0 and $w_{\rm ytr}$.

Once it is on the y-slow manifold $w = p(y, z)$, the z-dynamics takes over, sending the singular orbit (orbit 5) to the trivial z-nullcline on $w = p(y, 0)$ with $w = w_0 = w_{\rm ypd}|_{\{z=z_{\rm znl}\}}$. The slow w-dynamics takes over subsequently, moving the orbit upward (orbit 6). Notice that the nontrivial z-nullcline is in Δ because of conditions (3, 4). If we assume for the moment that it also lies about the y-fold curve as depicted in Fig.5(c), then the nontrivial z-nullcline strikes through the y-slow manifold $w = p(y, z)$ from $y = 0$ to $z = 0$. As a result it intersects on $w = p(y, 0)$ at a z-PDLS point between $w = 0$ and $w = w_{\rm yfd}$ as shown in Fig.6(b) labelled with $w_{\rm znl}$. Also between $w = 0$ and the y-fold point there is no $xyzw$-equilibrium point because of the effecient predator assumption on w (condition (5)). We can conclude now that after its passing the z-transcritical point $w_{\rm znl}$ on $z = 0, w = p(y, 0)$, the z-dynamics becomes unstable. Pontryagin's delay of loss of stability takes place for orbit 6 so that sooner or later it will develop in the increasing direction of z (orbit 7).

We note that in Fig.6(b), the y-fast orbits (1 and 4) are perpendicular to the drawing and hence they are hidden from the view.

To be more precise on how the singular orbit turns around in variable z, we again use the PDLS argument. Let $w_0 = w_{\rm ypd}|_{\{y=0,z=z_{\rm znl}\}}$ as above. Let $z_0 > 0$ be sufficiently near $z = 0$. A perturbed orbit starting from the plane $z = z_0$ at point (y_0, z_0, w_0) with y_0 defined by $w_0 = p(y_0, z_0)$ will eventually emerge away from $z = 0$ and strikes the plane $z = z_0$ in opposition direction. Let $w_{\rm zpd}$ denote the w-coordinate of the point of return. Then, the identity $0 = \int_{z_0}^{z_0} \epsilon_0 dz/z$ holds. Suppose the orbit does not pass the w-nullcline $y = y_{\rm wnl}$, then one substitution from variable z to w is sufficient to change the integral equation to

$$0 = \int_{z_0}^{z_0} \frac{\epsilon_0 dz}{z} = \int_{w_0}^{w_{\rm zpd}} \frac{\epsilon_0}{z}\frac{dz}{dw}dw = \int_{w_0}^{w_{\rm zpd}} \frac{h(q(y,z))}{wk(y)}dw. \tag{11}$$

Taking the double limit $\lim_{\epsilon_0\to 0}\lim_{\epsilon_2\to 0}$, the equation above becomes

$$0 = \int_{w_0}^{w_{\rm zpd}} \frac{h(q(y,0))}{wk(y)}dw = \int_{w_0}^{w_{\rm zpd}} \frac{h(q(p^{-1}(w),0))}{wk(p^{-1}(w))}dw,$$

with $y = p^{-1}(w)$ uniquely defined by the invertible function $w = p(y, 0)$.

Proposition 3. *If the z-PDLS point $w_{\rm zpd}$ defined by the equation above lies below the y-fold point $w_{\rm yfd}$, then there exists a singular yz-fast cycle.*

Proof. Take the interval $I = [w_{\rm ypd}, w_{\rm ytr}]$ on $z = 0, w = p(y, 0)$ as shown in Fig.6(b). A return map following the singular orbits of the interval can be defined. Under the assumption that $w_{\rm zpd}$ never surpasses the y-fold point $w_{\rm yfd}$, the lower end point $w_0 = w_{\rm ypd}$ returns to the interval I. Because the z-nullcline decreases in w with increase in z, we see clearly from Fig.6(b) that the upper end point $w_{\rm ytr}$ must also returns to I as well. The continuity of this return map is obvious. Also it is strictly increasing because of the way all PDLS points are defined by their respective integral equations whose solutions are unique. Hence there must be a unique fixed point of the return map, and the fixed point indeed corresponds to a yz-fast cycle. This completes the proof. □

The condition of this result must hold if the w is weak, and z is $xyzw$-competitive, as illustrated in Fig.6(a), i.e. the xyw-equilibrium point is unstable in the direction of z. As a result the z-PDLS point defined in the proposition will never pass the

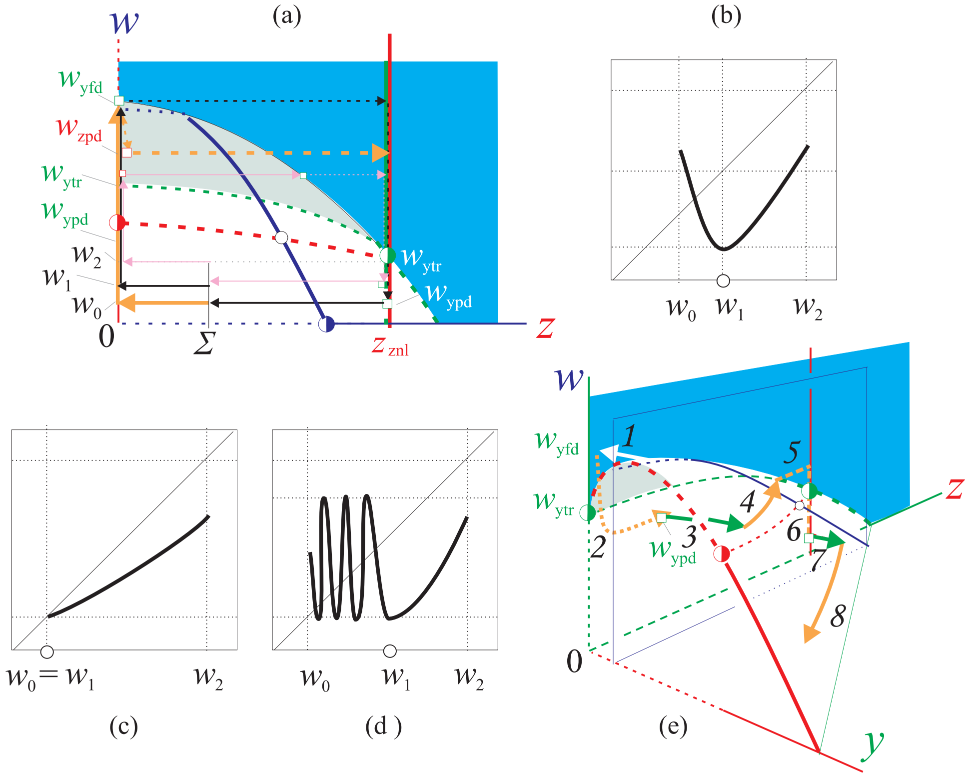

FIGURE 7. (a) The z-PDLS point corresponding to w_0 of Σ is at $w = w_{\rm zpd}$, lying on $y = z = 0$ after pushing over the y-fold point $w_{\rm yfd}$. (b) Due to the y-fold point $w_{\rm yfd}$ the return map π develops a local minimum at the pre-PDLS point w_1 of $w_{\rm zpd}$. (c) The bifurcation of the local minimum through $w_0 = w_1$. (d) Possible multiple extrema for small w_0. (e) Combination PDLS jumps on singular orbits with $\epsilon_2 = 0$.

unstable xyw-equilibrium point. In fact, the integral equation defining $w_{\rm zpd}$ above can be separated into two parts as

$$(12) \qquad 0 = \int_{w_0}^{w_{\rm zpd}} \frac{h(q(y,0))}{wk(y)} dw = \int_{w_0}^{w_{\rm znl}} \frac{h(q(y,0))}{wk(y)} dw + \int_{w_{\rm znl}}^{w_{\rm zpd}} \frac{h(q(y,0))}{wk(y)} dw,$$

with $y = p^{-1}(w)$. The first integral is negative and finite. The second integral is positive. The denominator of the integrant of the latter $\frac{h(q(y,0))}{wk(y)} = \frac{h(q(p^{-1}(w),0))}{wk(p^{-1}(w))}$ diverges as w increases to $w_{\rm wnl}$ at which $k(p^{-1}(w)) = 0$. Hence the integral equation above must have a solution for $w_{\rm zpd} < w_{\rm yfd}$ as required by Proposition 3's assumption.

Singular Chaotic Attractor and Return Map. Under the conditions of the main theorem that w is efficient, z is $xyzw$-competitive, fast y, slow z, and slower w, the xyw-equilibrium point is xyw-unstable, the xyw-cycle is $xyzw$-unstable. We start from the integral equation (11), $0 = \int_{z_0}^{z_0} \epsilon_0 dz/z$, that defines the z-PDLS point $w_{\rm zpd}$ starting at w_0. Recall that the assumption that the perturbed orbit from w_0

on $w = p(y, z)$ never crosses the w-nulllcline plane $y = y_{\rm wnl}$ gives rise to the integral equation (11). Now suppose instead that the orbit crosses the w-nullcline only once with w-coordinate at the crossing as w^*. Then the orbit is increasing in w from w_0 to w^* and decreasing from w^* to $w_{\rm zpd}$. Then two separate substitutions from z to w are needed to bring the equation $0 = \int_{z_0}^{z_0} \epsilon_0 dz/z$ into

$$\begin{aligned} 0 &= \int_{w_0}^{w^*} \frac{\epsilon_0}{z}\frac{dz}{dw}dw + \int_{w^*}^{w_{\rm zpd}} \frac{\epsilon_0}{z}\frac{dz}{dw}dw \\ &= \int_{w_0}^{w^*} \frac{h(q(y,z))}{wk(y)}dw + \int_{w^*}^{w_{\rm zpd}} \frac{h(q(y,z))}{wk(y)}dw. \end{aligned}$$

Although the two integrals look the same in form, the limiting behaviors with $\epsilon_2 \to 0$ are different. In the first integral all points lie on the nontrivial y-slow manifold $w = p(y, z)$ as $\epsilon_2 \to 0$. In the second all points lie on the trivial y-slow manifold $y = 0$ instead. Moreover, the y-fast dynamics forces $w^* \to w_{\rm yfd}$. Follow it up by taking $\epsilon_0 \to 0$, then $z = 0$ in both integrals. Therefore, with the double limit $\lim_{\epsilon_0 \to 0} \lim_{\epsilon_2 \to 0}$, the integral equation becomes

$$\begin{aligned} 0 &= \int_{w_0}^{w_{\rm yfd}} \frac{h(q(y,0))}{wk(y)}dw + \int_{w_{\rm yfd}}^{w_{\rm zpd}} \frac{h(q(0,0))}{wk(0)}dw \\ &= \int_{w_0}^{w_{\rm znl}} \frac{h(q(y,0))}{wk(y)}dw \\ &\quad + \left[\int_{w_{\rm znl}}^{w_{\rm yfd}} \frac{h(q(y,0))}{wk(y)}dw + \int_{w_{\rm yfd}}^{w_{\rm zpd}} \frac{h(q(0,0))}{wk(0)}dw\right] \\ &:= I_1 + I_2, \end{aligned} \tag{13}$$

breaking the integral from w_0 to $w_{\rm yfd}$ the same way as in (12) and having $y = p^{-1}(w)$ defined from $w = p(y, 0)$ as before. Here we have regrouped the integrals so that $I_1 = \int_{w_0}^{w_{\rm znl}} \frac{h(q(y,0))}{wk(y)}dw$ and I_2 equal the two integrals in the bracket. See Figs.6(b), 7(a). Notice that I_1 is negative which can diverge to $-\infty$ if $w_0 \to 0$. Whereas I_2 is positive, bounded above. This analysis implies that the condition of Proposition 3 must bifurcates into such a situation prescribed by equation (13) as $w_0 = w_{\rm ypd}|_{\{y=0,z=z_{\rm znl}\}}$ drops lower.

If we let Σ be a w-interval on $w = p(y, z)$ as shown in Fig.7(a) whose w-end points are the same as the interval $I = [w_{\rm ypd}, w_{\rm ytr}]$ from the proof of Proposition 3. For simpler notation let $w_2 = w_{\rm ytr}|_{\{y=0,z=z_{\rm znl}\}}$ and let w_1 be the pre-PDLS point of the y-fold $w_{\rm yfd}$, i.e. $\int_{w_1}^{w_{\rm yfd}} \frac{h(q(y,0))}{wk(y)}dw = 0$. It exists because we assume the z-PDLS point corresponding to w_0 is pushed over the y-fold and lie on the w-axis as shown in Fig.7(a). Then the same singular orbit induced return map used in the proof Proposition 3 is no longer monotone increasing. Let π denote the return map. Then w_1 is a critical point in $\Sigma = [w_0, w_2]$. It increases in $[w_1, w_2]$ and decreases in $[w_0, w_1]$ as depicted in Fig.7(b). Fig.7(c) shows the case at bifurcation when $w_0 = w_1$.

If w_0 is just slightly perturbed below the bifurcation point $w_0 = w_1$, then the z-PDLS point $w_{\rm zpd}$ is perturbed slightly below $w_{\rm yfd}$, and the image $\pi(w_0)$ of the return map lies a little bit above w_0. Further decreasing w_0 will result in significant increase in $\pi(w_0)$, which may give rise to chaotic dynamics of the return map π. Decreasing w_0 further can make the return map more complex by creating more critical points as shown in Fig.7(d). In fact, decreasing w_0 makes the negative integral I_1 of (13) more negative. To counter balance I_1, $w_{\rm zpd}$ must further move downward on the w-axis and come to meet the y-PDLS point $w_{\rm ypd}$. At this point the y-fast dynamics must take over to switch the singular orbit to the stable y-slow manifold $w = p(y, z)$. Further decreasing w_0 moves the $w_{\rm zpd}$ upwards on the nontrivial stable y-nullcline $w = p(y, 0)$, splitting the integral I_2 further into three parts

$$I_2 = \int_{w_{\rm znl}}^{w_{\rm yfd}} \frac{h(q(y,0))}{wk(y)}dw + \int_{w_{\rm yfd}}^{w_{\rm ypd}} \frac{h(q(0,0))}{wk(0)}dw + \int_{w_{\rm ypd}}^{w_{\rm zpd}} \frac{h(q(y,0))}{wk(y)}dw. \tag{14}$$

Under this situation, another critical point emerges between w_0 and w_1 to become a local maximum for the return map π. Now it is clear to see that further decreasing w_0 will make the z-PDLS point $w_{\rm zpd}$ to move up on $w = p(y, 0)$ and down on $y = z = 0$, creating more local extrema. Fig.7(d) shows such a possible situation.

Depending on the location of w_0, the singular orbit may cycle around the xyw-cycle several times before hitting its z-PDLS point. This conclusion is based on the property that the z-competitive condition and the calculation of the z-PDLS point are essentially the same type of integrals as above. To be precise, let $(y_c(t), 0, w_c(t))$ denote the perturbed cycle for $\epsilon_2 > 0$, and T be the period. Then z is xyw-competitive if $J = \int_0^T h(q(y_c(t), 0))dt > 0$. Let $t = 0$ correspond to the w-minimum value w_* on the w-nullcline on $z = 0$ and let $t = T_1$ correspond to the w-maximum point with w^*. Then w is increasing from w_* to w^* over $[0, T_1]$ and decreasing from w^* to w_* over $[T_1, T]$. Split the integral over $[0, T_1]$ and $[T_1, T]$ and use the substitution $dt = dw/wk(y_c(t))$ to get

$$J = \int_{w_*}^{w^*} \frac{h(q(y_c, 0))}{wk(y_c)}dw + \int_{w^*}^{w_*} \frac{h(q(y_c, 0))}{wk(y_c)}dw,$$

with the integrants tracing along the two half of the cycle. In limit $\epsilon_2 \to 0$, $\lim w^* = w_{\rm yfd}$ and $\lim w_* = w_{\rm ypd}$, and $y_c = p^{-1}(w)$ for the first integral and $y_c = 0$ for the second integral, and

$$J_0 = \lim_{\epsilon_2 \to 0} J = \int_{w_{\rm ypd}}^{w_{\rm yfd}} \frac{h(q(p^{-1}(w), 0))}{wk(p^{-1}(w))}dw + \int_{w_{\rm yfd}}^{w_{\rm ypd}} \frac{h(q(0, 0))}{wk(0)}dw > 0,$$

the same type of integrals as for the z-PDLS integral in (14) above. In particular, the integral equation (12) for the z-PDLS point can be broken down to the sum of an integral from w_0 to $w_{\rm ypd}$, an integer multiple of J_0, and a remainder part from $w_{\rm ypd}$ to $w_{\rm zpd}$. The first and the last integrals together is precisely the same form of the z-PDLS integral equation (13) described above, except to break (13) differently at $w_{\rm ypd}$ instead of at $w_{\rm yfd}$. Because $J_0 > 0$, singular solutions always jump away from the cycle no mater where they start at $w_0 > 0$.

One sufficient condition for chaotic dynamics is to have three adjacent critical points that straddle the diagonal $\pi = w$ in the sense that the value of the middle point under the return map is on one side of the diagonal $\pi = w$ and those of the other two are on the opposite side of the diagonal. More precisely we have the following partial result. Also, multiple bumps must occur on the graph of π if w_0 is sufficiently small and the singular orbit cycles around the xyw-cycle several times before jumping away in the z-direction.

Proposition 4. *If there exist three adjacent critical points of π that straddle the diagonal, then there is a subset of Σ on which π is equivalent to the shift dynamics on two symbols.*

Proof. A proof for such a continuous map is given in [8]. □

Numerical simulations indeed suggest such a scenario of Proposition 4, e.g. Fig.4, as well as chaos due to the existence of a single critical point for a quadratic-like map π.

Finally we conclude this subsection by explaining a special case of Pontryagin's delay of loss of stability when the slow flow is 2-dimensional. The ϵ_2-fast dynamics is that of y, and the ϵ_2-slow dynamics is that of z, w. Start a point on the y-fold as shown in Fig.7(e). The singular ϵ_2-fast dynamics sends it down on $y = 0$ (orbit 1). The ϵ_2-slow zw-dynamics takes over (orbit 2). It moves down in w, crosses the y-transcritical curve, and jumps back to $w = p(y, z)$ at some y-PDLS point w_{ypd} as shown (orbit 3), and zigzags its way toward $y = 0, z = z_{\text{znl}}$ afterward (orbit 4 and 5 when 4 lies above the z-nullcline $(y_{\text{znl}}, z_{\text{znl}}, w_{\text{znl}})$). Since we always pick nonzero singular values $0 < \epsilon_2 \ll \epsilon_1 \ll 1$ for numerical simulations, such zigzag orbits are bound to occur as shown in Fig.4 which is the case when the w_{ypd} values lie below the corresponding w_{znl} on the y-nullcline $w = p(y, z)$.

Acknowledgement: The authors would like to thank the reviewer for his/her invaluable comments and suggestions.

References

1. Armstrong, R.A. and R. McGehee, *Competitive exclusion,* Amer. Naturalist, **115**(1980), pp.151–170.
2. Bonet, C., *Singular perturbation of relaxed periodic orbits,* J.D.E., **66**(1987), pp.301–339.
3. Calder III, W.A., *An allometric approach to population cycles of mammals,* J. Theor. Biol., **100**(1983), pp.275-282.
4. Calder III, W.A., *Ecological scaling: mammals and birds,* Ann. Rev. Ecol. Syst., **14**(1983), pp.213-230.
5. Deng, B., *Glucose-induced period-doubling cascade in the electrical activity of pancreatic β-cells,* J. Math. Bio., **38**(1999), pp.21–78.
6. Deng, B., *Food chain chaos due to junction-fold point,* Chaos, **11**(2001), pp.514–525.
7. Deng, B. and G. Hines, *Food chain chaos due to Shilnikov orbit,* Chaos, **12**(2002), pp.533–538.
8. Deng, B. and G. Hines, *Food chain chaos due to transcritical point,* Chaos, **13**(2003), pp.578–585.
9. Eckhaus, W., *Relaxation oscillations including a standard chase on French ducks,* in Asymptotic analysis II, Springer Lecture Notes Math. **985**(1983), pp.449–494.
10. Fenichel, N., *Geometric singular perturbation theory for ordinary differential equations*, J. Diff. Eqns., **31**(1979), pp.53–98.
11. Holling, C.S., *Some characteristics of simple types of predation and parasitism,* the Canadian Entomologist, **91**(1959), pp.385–398.
12. Koch, A.L., *Competitive coexistence of two predators utilizing the same prey under constant environmental conditions,* J. Theor. Biol., **44**(1974), pp.373–386.
13. Liu, W., D. Xiao, and Y. Yi, *Relaxation oscillations in a class of predator-prey systems,* J.D.E., **188**(2003), pp.306–331.
14. Loladze, I., Y. Kuang, J.J. Elser, and W.F. Fagan, *Competition and stoichiometry: coexistence of two predators on one prey,* Theor. Pop. Bio., **65**(2004), pp.1–15.
15. Loladze, I., personal communication.
16. Lotka, A.J., *Elements of Physical Biology,* Williams and WWilkins, Baltimore, Md., 1925.
17. Mishchenko, E.F., Yu.S. Kolesov, A.Yu. Kolesov, and N.Kh. Rozov, Asymptotic Methods in Singularly Perturbed Systems, Monographs in Contemporary Mathematics, Consultants Bureau, New York, 1994.

18. Muratori, S. and S. Rinaldi, *Low- and high-frequency oscillations in three-dimensional food chain system,* SIAM J. Appl. Math., **52**(1992), pp.1688–1706.
19. O'Malley, Jr., R.E., Introduction to Singular Perturbations, Academic Press, New York, 1974.
20. Pontryagin, L.C., *Asymptotic behavior of solutions of systems of differential equations with a small parameter at higher derivatives,* Izv. Akad. Nauk. SSSR Ser. Math. **21**(1957), pp.605-626 (in Russian).
21. Schecter, S., *Persistent unstable equilibria and closed orbits of a singularly perturbed equation,*J. Diff. Eq., **60**(1985), pp.131–141.
22. Verhulst, P.F., *Notice sur la loi que la population suit dans son accroissement,*Corr. Math. et Phys. **10**, pp.113-121(1838).
23. Volterra, V., *Fluactuations in the abundance of species, considered mathematically,* Nature, **118**(1926), pp.558–560.
24. Waltman, P., Competition Models in Population Biology, SIAM, Philadelphia, 1983.

Appendix A: Analytical Equivalence of YZ-Weakness: Analytically, we can parametrically represent the manifold,

$$f(x,y,z) = 1 - x - \frac{y}{\beta_1 + x} - \frac{z}{\beta_2 + x} = 0,$$

which is linear both in y and z, as

$$\begin{array}{c} y = \alpha(1-x)(\beta_1 + x), \quad z = (1-\alpha)(1-x)(\beta_2 + x) \\ \text{for } 0 \le x \le 1 \text{ and } 0 \le \alpha \le 1, \end{array} \tag{15}$$

with the introduction of parameter α. The x-fold curve is where the manifold $f(x,y,z) = 0$ comes in tangent to the horizontal x-fast flow lines. It necessarily satisfies these two equations $f(x,y,z) = 0, f_x(x,y,z) = 0$ simultaneously as we have already pointed out earlier Using the parametrization (15) again together with the additional equation

$$f_x(x,y,z) = -1 + \frac{y}{(\beta_1 + x)^2} + \frac{x}{(\beta_2 + x)^2} = 0,$$

we obtain after eliminating the parameter α the x-fold curve:

$$\begin{array}{c} y = \dfrac{(2x - 1 + \beta_2)(\beta_1 + x)^2}{\beta_2 - \beta_1} \\ z = \dfrac{(2x - 1 + \beta_1)(\beta_2 + x)^2}{\beta_1 - \beta_2} \\ \text{for } \dfrac{1 - \max\{\beta_1, \beta_2\}}{2} < x < \dfrac{1 - \min\{\beta_1, \beta_2\}}{2}, \quad \beta_2 \ne \beta_1; \end{array} \tag{16}$$

and if $\beta_1 = \beta_2$, then

$$x = \frac{1 - \beta_1}{2}, \quad y + z = \frac{(1 + \beta_1)^2}{4}.$$

(Note also that the special cases for the xy-fold point and the xz-fold point are, respectively, $x = (1-\beta_1)/2, y = (1+\beta_1)^2/4, z = 0$ and $x = (1-\beta_2)/2, y = 0, z = (1+\beta_2)^2/4$ as expected.) Because the x-fold ranges in x only in the interval $(1 - \max\{\beta_1, \beta_2\})/2 < x < (1 - \min\{\beta_1, \beta_2\})/2$ by (16) and recall that $x_{\text{xfd}}|_{\{z=0\}} = (1-\beta_1)/2, x_{\text{xfd}}|_{\{y=0\}} = (1-\beta_2)/2$, the condition that the predators nullcline planes, $x = x_{\text{ynl}} = \frac{\beta_1\delta_1}{1-\delta_1}$, $x = x_{\text{znl}} = \frac{\beta_2\delta_2}{1-\delta_2}$, lie above the crash fold holds iff both $x_{\text{ynl}}, x_{\text{znl}}$ are greater than both the x_{xfd} values. This gives the analytical yz-weak condition stated in (7).

Appendix B: Existence of Y-Fold:

Proposition 5. *Under conditions:*

$$\max\{\frac{1-\beta_i}{2}\} < \min\{\frac{\beta_i\delta_i}{1-\delta_i}\} \text{ and } \beta_3 < \frac{(\beta_1+1)^3}{\beta_1}\left(\frac{1}{\beta_1+1}-\delta_1\right)$$

there is a unique y-fold curve $p_y(y,z)=0$ *in* Δ *from* $z=0$ *to* $y=0$, *and* $p_y(0,0)>0$, $p_y(y,z)<0$ *for* $q(y,z)=x_{\rm ynl}$.

Proof. The idea is to show that along any radius line $y=s, z=ms$ in the first quadrant $m\ge 0, s\ge 0$ from the origin $(0,0), s=0$ to the Δ boundary $q(s,ms)=x_{\rm ynl}$, there is a unique zero for the function $w_y=p_y(s,ms)$.

With $x=q(y,z)\in[x_{\rm ynl},1]$ below, the y-partial derivative of w is

$$\begin{aligned} w_y =& p_y(y,z) = \frac{\beta_1}{(\beta_1+x)^2}q_y(\beta_3+y)+\left(\frac{x}{\beta_1+x}-\delta_1\right)\\ =&\frac{\beta_1}{(\beta_1+x)^2}\left(-\frac{f_y}{f_x}\right)(\beta_3+y)+\left(\frac{x}{\beta_1+x}-\delta_1\right)\\ =&\left(-\frac{f_y(\beta_1+x)}{f_x}\right)\left[\frac{\beta_1}{(\beta_1+x)^3}(\beta_3+y)+\left(-\frac{f_x}{f_y(\beta_1+x)}\right)\left(\frac{x}{\beta_1+x}-\delta_1\right)\right]\\ =&\frac{1}{f_x}\left[\frac{\beta_1}{(\beta_1+x)^3}(\beta_3+y)+f_x\left(\frac{x}{\beta_1+x}-\delta_1\right)\right] \text{ (since } f_y=-\tfrac{1}{\beta_1+x}) \end{aligned}$$

Since $f_x=-1+\frac{y}{(\beta_1+x)^2}+\frac{z}{(\beta_3+x)^2}=-1$ at $x=1, y=z=0, s=0$, we have immediately

$$\begin{aligned} w_y|_{\{x=1,y=z=0\}} &= -\left[\frac{\beta_1\beta_3}{(\beta_1+1)^3}-\left(\frac{1}{\beta_1+1}-\delta_1\right)\right]\\ &=-\frac{\beta_1}{(\beta_1+1)^3}\left[\beta_3-\frac{(\beta_1+1)^3}{\beta_1}\left(\frac{1}{\beta_1+1}-\delta_1\right)\right]>0 \end{aligned}$$

by the assumption on β_3. Also, at $x=q(s,ms)=x_{\rm ynl}=\beta_1\delta_1/(1-\delta_1)$,

$$w_y|_{\{x=x_{\rm ynl}\}}=\left(\frac{1}{f_x}\right)\frac{\beta_1}{(\beta_1+x)^3}(\beta_3+y)<0$$

because $f_x<0$ in $\mathcal{S}$ by definition. Therefore there must a zero of $w_y=p(s,ms)$ between $s=0$ and $q(s,ms)=x_{\rm ynl}$. So it is only left to show that the zero is unique.

To this end, we make a simple change of variable $x=q(s,ms)$ so that x runs from 1 to $x_{\rm ynl}$ with increasing s from $s=0$. Since $x_s=q_y+mq_z<0$ because both $q_y,q_z<0$ and $m\ge 0$, this is a valid substitution. Moreover, the inverse $s=s(x)$ is well defined, and is monotone decreasing: $s_x<0$. Denote

$$w_y=\frac{1}{f_x}\left[\frac{\beta_1}{(\beta_1+x)^3}(\beta_3+y)+f_x\left(\frac{x}{\beta_1+x}-\delta_1\right)\right]:=\frac{1}{f_x}Q(x).$$

Then we know $Q(1)<0, Q(x_{\rm ynl})>0$, and we only need to show $Q'(x)<0$ for $x\in[x_{\rm ynl},1]$. Writing Q out

$$Q(x)=\frac{\beta_1}{(\beta_1+x)^3}(\beta_3+s(x))+\left(-1+\frac{s(x)}{(\beta_1+x)^2}+\frac{ms(x)}{(\beta_3+x)^2}\right)\left(\frac{x}{\beta_1+x}-\delta_1\right)$$

we see that $Q'(x)<0$. In fact, the first term is obviously decreasing in x. The second term is the product of two factors: $a(x)b(x):=f_x(\frac{x}{\beta_1+x}-\delta_1)$. By product rule, we have $a'(x)b(x)+a(x)b'(x)$. Since $a=f_x$ is negative, decreasing, and b

is positive, increasing, we see clearly that it is decreasing for the product. This completes the proof. □

Appendix C: Nullclines of $XYZW$-Web: The attracting branch of the nontrivial x-nullcline satisfies $f_x(x,y,z) < 0$ by definition. Therefore it can be solved from $f(x,y,z) = 1 - x - \frac{y}{\beta_1+x} - \frac{z}{\beta_2+x} = 0$ by Implicity Function Theorem in terms of x as a function $x = q(y,z)$ of y,z. Because it is independent of w, the manifold is a solid or hyper-surface in the $xyzw$-space, parallel to the w-axis, which we denote by $\mathcal{S} : x = q(y,z)$ for points (y,z) interior to the fold surface (16). Since $f_x < 0$ on $\mathcal{S}$, and $f_y < 0, f_z < 0$, we have that $q_y = -f_y/f_x < 0$ and $q_z = -f_z/f_x < 0$. Hence, q decreases in both y and z variables, with $q(0,0) = 1$. When projected to the yzw-space, $\mathcal{S}$ is a cylindrical solid in the first yzw-octant, bounded by the coordinate planes and the fold cylindrical surface (16). In other words, it is the domain of definition in the positive yzw-octant for the function q. We will use the same notation S for its yzw-projection solid.

Eq.(9) is again singularly perturbed by parameters $0 < \epsilon_i \ll 1$. The zw-plane $(y = 0)$ is always the trivial y-nullcline. The intersection of the nontrivial y-nullcline within $\mathcal{S}$ is determined by the system of equations $f(x,y,z) = 0, g(x,y,w) = 0$, which is expressed as

$$w = p(y,z) := \left(\frac{q(y,z)}{\beta_1 + q(y,z)} - \delta_1 \right) (\beta_3 + y),$$

with (y,z) constraint to the region $\Delta := \{\frac{q(y,z)}{\beta_1+q(y,z)} - \delta_1 \geq 0, y \geq 0, z \geq 0\}$, equivalently $\Delta = \{q(y,z) \geq \beta_1\delta_1/(1-\delta_1) = x_{\text{ynl}}, y \geq 0, z \geq 0\}$. It is a surface in the x-slow manifold solid $\mathcal{S}$. Since q is decreasing in y,z, and the boundary curve $x = q(y,z) = x_{\text{ynl}}$ is a line, obvious from the defining equation $f(x,y,z) = (1 - x - y/(\beta_1 + x) - z/(\beta_2 + x) = 0$, therefore the domain of definition Δ for the y-nullcline $w = p(y,z)$ in $\mathcal{S}$ is a triangle bounded by the axises $y = 0, z = 0$ and the line $q(y,z) = x_{\text{ynl}}$, see Fig.5.

The y-transcritical curve is given by $w = p(0,z) = (\frac{x}{\beta_1+x} - \delta_1)\beta_3$ with $x = q(0,z)$ which satisfies $z = (1-x)(\beta_2 + x)$, with z between 0 and $z = (1 - x_{\text{ynl}})(\beta_2 + x_{\text{ynl}})$. It is monotone decreasing in z. In fact, $w_z = p_z(0,z) = \frac{\beta_1\beta_3}{(\beta_1+x)^2} x_z$ whose sign is the same as $1/x_z = z_x = 2(\frac{1-\beta_2}{2} - x) < 0$ because $x \geq x_{\text{ynl}} > x_{\text{xfd}}|_{\{y=0\}} = (1-\beta_2)/2$ by the y-weak assumption.

As we mentioned earlier in Sec.5 that the xyw-system with $z = 0$ has a unique y-nullcline fold point on the stable x-manifold $f = 0$, and it is a special case of Proposition 5. More specifically, a fold turning point for the y-flow in the solid $\mathcal{S}$ is determined by $g_y(q(y,z),y,w) = 0, g(q(y,z),y,w) = 0$. In terms of $w = p(y,z)$ for the y-nullcline in $\mathcal{S}$: $g(q(y,z),y,w) = 0$, the condition $g_y(q(y,z),y,w) = 0$ is equivalent to $w_y = p_y(y,z) = -g_y(q(y,z),y,w)/g_w(q(y,z),y,w) = 0$. Also, the stable branch of the y-nullcline is determined by $g_y(q(y,z),y,w) < 0$, which is equivalent to $w_y = p_y(y,z) < 0$ because $g_w < 0$ always.

Proposition 5 proves that the y-nullcline surface $w = p(y,z)$ in $\mathcal{S}$ indeed has a unique y-fold curve $w_y = p_y(y,z) = 0$ on $w = p(y,z)$ running from Δ's boundary $z = 0$, which is the above special case, to another boundary $y = 0$. Denote this fold curve by $(y,z,w)_{\text{yfd}}$. This curve divides the y-nullcline into the stable branch and the unstable branch. The unstable part contains the y-transcritical point, in particular $x = 1, y = z = 0, w = q(0, 0)$, and the stable part contains the boundary $q(y, z) = x_{\rm ynl}$, see Proposition 5.

The nontrivial z-nullcline $h(x) = 0$ in the x-slow manifold solid $f(x, y, z) = 0$ is given by $x = x_{\rm znl}, f(x, y, z) = 1 - x - y/(\beta_1 + x) - z/(\beta_2 + x) = 0$. It is a line in the yz-plane and a plane parallel to the w-axis in the solid $\mathcal{S}$. Important properties about it include the following:

(1) If z is competitive ($E_{xy} = x_{\rm ynl} - x_{\rm znl} > 0$), then the z-nullcline $x = x_{\rm znl}$ does not intersect the y-slow manifold $w = p(y, z) = (\frac{x}{\beta_1+x} - \delta_1)(\beta_3 + y)$ since $w < 0$ with $x = x_{\rm znl}$. On the yz-plane in $\mathcal{S}$, the line $x = x_{\rm znl}$ lies between the x-fold curve and the boundary line $x = q(y, z) = x_{\rm ynl}$ for for the y-slow manifold $w = p(y, z)$. See Fig.5.

(2) If z is not competitive ($E_{xy} = x_{\rm ynl} - x_{\rm znl} < 0$), then the z-nullcline $x = x_{\rm znl}$ intersects the y-slow manifold $w = p(y, z) = (\frac{x}{\beta_1+x} - \delta_1)(\beta_3 + y)$ in the solid $\mathcal{S} : f(x, y, z) = 1 - x - y/(\beta_1 + x) - z/(\beta_2 + x) = 0$ along a line

$$w = p(y, z) = \left(\frac{x}{\beta_1 + x} - \delta_1\right)(\beta_3 + y), \quad z = (\beta_2 + x)\left(1 - x - \frac{y}{\beta_1 + x}\right)$$

parameterized by $y \in [0, (1 - x)(\beta_1 + x)]$, with $x = x_{\rm znl}$ above. Along it w increases while z decreases with increase in y. We denote this line by $(y, z, w)_{\rm znl}$.

(3) The z-transcritical line is given by the intersection of the trivial z-nullcline $z = 0$ and $x = x_{\rm znl}$ in the solid $\mathcal{S} : f(x, y, z) = 1 - x - y/(\beta_1 + x) - z/(\beta_2 + x) = 0$, which is the line $y_{\rm ztr} = (1 - x_{\rm znl})(\beta_1 + x_{\rm znl})$. Point $(y_{\rm ztr}, 0, w_{\rm ztr}) = (y_{\rm ztr}, 0, p(y_{\rm ztr}, 0))$ is the z-transcritical point on the y-slow manifold $w = p(y, z)$. See Fig.5.

Finally, the nontrivial w-nullcline ($k(y) = 0$) is given by the hyper-plane

$$y = y_{\rm wnl} = \frac{\beta_3\delta_3}{1 - \delta_3}.$$

It intersects the y-slow manifold $w = p(y, z)$ in $\mathcal{S}$ along a curve $w = p(y_{\rm wnl}, z)$ with z from 0 to $z_{\rm wnl} = (1 - x_{\rm ynl} - y_{\rm wnl}/(\beta_1 + x_{\rm ynl}))(\beta_2 + x_{\rm ynl})$, which is the intersection of $y = y_{\rm wnl}$ with the boundary $w = 0, q(y, z) = x_{\rm ynl}$. This w-nullcline will intersect the y-fold curve if w is efficient as defined in Sec.6, or may not if w is weak as shown in Fig.5. The point $(y_{\rm wnl}, z_{\rm wnl}, w)$ is the w-transcritical point on the y-slow manifold $w = p(y, z)$.

Department of Mathematics, State University of West Georgia Carrollton GA, 30118

Department of Mathematics & Statistics, University of Nebraska-Lincoln, Lincoln, NE68588-0323. Contact bdeng@math.unl.edu for correspondence.

Department of Mathematics & Statistics, University of Nebraska-Lincoln, Lincoln, NE68588-0323

Department of Mathematics & Statistics, University of Nebraska-Lincoln, Lincoln, NE68588-0323

Department of Mathematics, California State University at Fullerton/Iowa State University, Ames, IA 50011

Department of Mathematics, Kent State University, Kent, OH 44240